SIMULATION OF THE FERMILAB MAIN INJECTOR DIGITAL DAMPERS AND COMPARISON WITH BEAM TEST RESULTS

Dennis J. Nicklaus

Submitted to the faculty of the University Graduate School

in partial fulfillment of requirements

for the degree

Master of Science

in the Department of Physics,

Indiana University

April 2004

Accepted by the Graduate Faculty, Indiana University in partial fulfillment of the requirements for the degree of Master of Science.

_____

Dr. SY Lee, committee chair

_____

Dr. Michael W. Snow

Masters

Committee

_____

Dr. Rex Tayloe

April 26, 2004

Acknowledgements

I'm very grateful to everyone who has made this work possible. First and foremost, thank you to my wonderful wife, Sherry, and our daughters Liana and Athena for their patience while I was off to particle accelerator school for two weeks at a time. Thank you to Professor SY Lee of Indiana University for his encouragement and help through this thesis project and the USPAS experience. Also, Susan Winchester of the Fermilab USPAS office has provided lots of support and help in interacting with IU for me. I'm thankful to Bill Foster for his development of the Main Injector damper project which made all this thesis project possible, and also for his support and suggestions in defining this thesis work. I'd also like to say thanks to all the people at Fermilab and the DOE with a hand in creating and supporting the US Particle Accelerator School, in particular my immediate supervisors and coworkers who have supported my attendance at USPAS courses.

Abstract

Dennis J. Nicklaus

Simulation of the Fermilab Main Injector Digital Dampers and Comparison With Beam Test Results

The resistive wall instability of the Fermilab Main Injector accelerator has been simulated using rigid bunch approximations of a beam signal. This simulation is compared with experimental measurements acquired with a digital data acquisition system. Further simulation models the behavior of the Main Injector transverse damper system. Characteristics of the damper system firmware are directly implemented in the simulation to ensure a good comparison. The simulation predicts the current damper system is able to support the design intensity goals for the Main Injector during Fermilab's Run II.

Contents

List of Figures

Chapter 1

Introduction

In order to understand the way objects move in the real world, a beginning physics student must move beyond ideal, frictionless approximations when calculating velocities using Newton's laws and begin accounting for interactions with the environment such as friction or the stretching of a rope pulling a weight. Similarly, to understand, design, and operate synchrotron particle accelerators, one must advance beyond ideal assumptions and calculations of beam orbits and account for interactions between the particle beam and its environment. One such interaction comes from the conducting walls of the accelerator beam pipe for a typical particle beam.

The interaction between the beam and beam pipe is the *resistive wall* effect, so called because the beam pipe walls have a non-zero electrical resistivity. As a first step in understanding the evolution of the resistive wall effects in a circulating beam, this interaction has been modeled and simulated for the Fermilab Main Injector. The results of this simulation are compared with beam measurements to gauge the utility and correctness of the simulation and to verify explanations for behavior seen in the beam measurements.

This simulation is only a first-step toward modeling the beam-to-environment

interactions. In the Main Injector, as in all synchrotron particle accelerators, the particles of the circulating beam are grouped into bunches, rather than having a continuous uniform beam. The simulation presented here is a *rigid bunch* simulation. "Rigid bunch" means that a bunch of particles is treated as one single lumped charge. The simulation ignores any effects caused by having a finite sized beam with multiple particles distributed in space. It also ignores interactions within the bunch of particles, any space charge effects (direct EM forces between the particles in a beam), and evolution of transverse and longitudinal bunch shape.

The following chapter of this thesis contains a brief review of some of the accelerator physics concepts underlying the simulation and work. Chapter 3 discusses the facilities and equipment involved in the project and details about the simulation setup. Chapter 4 presents some of the results of the simulation and Chapter 5 contains further results related to the damping process. After that are a few concluding remarks and an Appendix showing some of the steps taken to calibrate and verify the correctness of the simulation.

Chapter 2

Accelerator Physics Review

2.1   Review of Impedance

To understand the interactions between a particle beam and its environment (beam pipe walls, accelerating cavities, baffles, etc.) it is helpful to introduce the concept of impedance[12].

To briefly introduce impedance, it is helpful to start at Ohm's law for DC circuits: $V = IR$, where V is the voltage across a resistor, I is the current, and R is the electrical resistance. For an AC current, the simple resistance R must be replaced by the complex impedance, Z, which is defined as $Z = R + jX$ where the imaginary part X is the called the *reactance*. For example, in a series R, L, C electrical circuit, for a periodic current with frequency ω the impedance is defined as $Z(\omega) = R + j\omega L - \frac{j}{\omega C}$ where R is the resistance, C the capacitance and L the inductance. The impedance Z gives the relationship between the current and the electromotive force, or work done by the electric field. The work is done in the resistive heating (RI^2), changing energy in the magnetic field of the current $(LI^2/2)$, and changing the energy of the electric field $(q^2/2C)$.

There is also an impedance for a circulating charged particle beam, which can be separated into transverse and longitudinal components. In particle accelerators, the beam is moving in a vacuum, so there is no direct resistance. However, the beam excites electromagnetic fields which induce currents and voltages in the beam pipe walls. A beam's *coupling impedance* relates the beam current to the induced voltages on the beam trajectory. The induced voltage is defined as the integral over all the EM forces on the beam. A constant velocity beam moving through the beam pipe with some transverse (perpendicular to the axis of motion) offset from the center will experience electric forces in the direction of beam motion and magnetic forces perpendicular to it. These parallel and perpendicular forces produce the longitudinal and transverse impedances.

2.2   Resistive Wall Instability

As just mentioned, the circulating beam of charged particles is accompanied by electromagnetic waves. When the beam is off-center, it will induce an image current in the walls of the beam pipe. The electromagnetic field from the walls of the beam pipe, the *wakefield*, will linger after the particles causing it have passed. This induced electromagnetic field will exert a transverse force on the subsequent particles of the beam. These forces introduce coupling between bunches of a bunched beam and this feedback can lead to instability. The force on the particles from the induced magnetic fields is called the resistive wall impedance.

The transverse effects of the resistive wall impedance on a typical beam at the Fermilab Main Injector have been simulated and several results of this simulation will be shown in later chapters.

2.3   Betatron Motion

The designed trajectory around the circumference of a synchrotron is called the *reference orbit*. In the simplest terms, one might think of the reference orbit as going right down the center of the beam pipe all around the circumference. In practice, the particles oscillate around the reference orbit and this motion is called *betatron oscillation*. The number of betatron oscillations per full orbit is called the *tune* of the particles. Tune is commonly represented by the symbol ν.

Figure 2.1 shows an orbit with $\nu = 4$, four full oscillations each revolution. Figure 2.2 shows an orbit with $\nu = 24.4$. Notice that the non-integral tune of 24.4 means that the particle doesn't come back to the repeat the same orbit after one revolution. These figures are only for illustrating the principles of tune and betatron motion. The amplitude of the betatron oscillation is greatly exaggerated relative to the circumference, and integer tunes such as 4, or tunes where the fractional part is a ratio of two integers such as the 0.4 in 24.4, will give rise to resonances which will prevent beam stability.

2.4   Propagation Matrices

To compute the propagation matrix for advancing x (the position offset) and x' (the rate of change of the position) from one station (location along the accelerator) to the next, the average beta function is used throughout the simulation. The simulation doesn't need to know the actual machine lattice. Thus beta is, on average, the same everywhere, equal to the $(circumference)/2\pi\nu$ and the phase advance angle ϕ is a constant $2\pi\nu/N_s$ (ν is the tune; N_s is the number of stations — 588 was chosen for this simulation). The propagation matrix becomes:
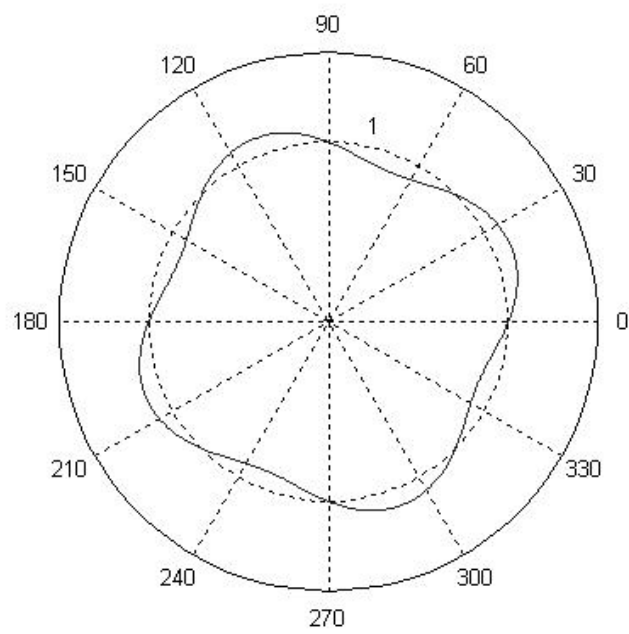
Figure 2.1: Schematic showing particle orbit with $\nu = 4$
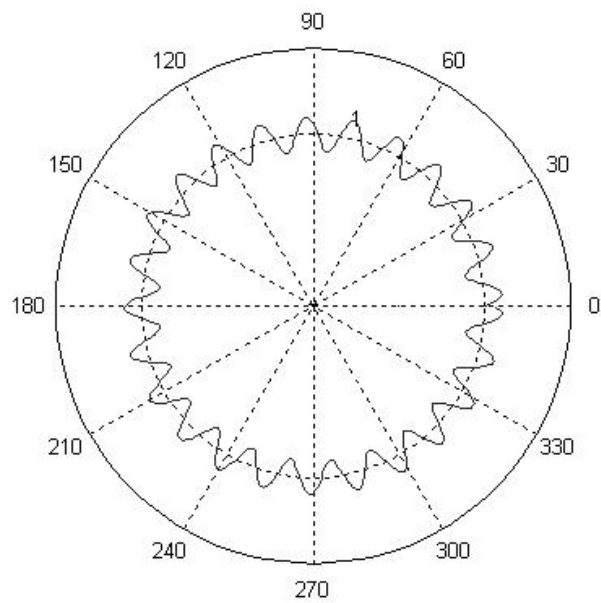
Figure 2.2: Schematic showing particle orbit with $\nu = 24.4$. Note discontinuity at $0\,\text{deg}$ due to non-integer tune value.

$$\begin{pmatrix} \cos(\phi) & \sin(\phi)\beta \\ -\sin(\phi)/\beta & \cos(\phi) \end{pmatrix}$$

This is easily derived from the standard propagation matrix[1]:

$$\begin{pmatrix} \sqrt{(\beta_2/\beta_1)}(\cos(\phi) + \alpha_1 \sin(\phi)) & \sqrt{(\beta_1\beta_2)}\sin(\phi) \\ -\frac{(1+\alpha_1\alpha_2)\sin(\phi)}{\sqrt{(\beta_1\beta_2)}} + \frac{(\alpha_1-\alpha_2)\cos(\phi)}{\sqrt{(\beta_1\beta_2)}} & \sqrt{(\beta_1/\beta_2)}(\cos(\phi) - \alpha_2 \sin(\phi)) \end{pmatrix}$$

where $\beta_2 = \beta_1$ and $\alpha_1 = \alpha_2 = 0$, since α is defined as

$$\alpha = -\frac{1}{2}\frac{d\beta}{ds}$$

and thus α is uniformly 0 with the condition of a constant β.

Chapter 3

Facilities and Experimental Equipment

This chapter describes our approach and equipment and provides some details of the simulation implementation.

3.0.1 Fermilab Main Injector

The Fermilab Main Injector is a synchrotron approximately 3319 meters in circumference, accelerating protons or anti-protons from 8 GeV/c to 150 GeV/c. A *synchrotron* is a circular particle accelerator where the magnetic field of the steering magnets is increased synchronously with the increase in particle energy as the particles are accelerated, in order to keep the particles orbiting the accelerator ring.

The Main Injector serves as an intermediate accelerator for Fermilab's Tevatron and also is used in anti-proton production and fixed target experiments.

The Main Injector circulates a bunched 53 MHz beam. Thus, the time between bunches is about 18.8ns and there are 588 buckets (bunch slots) available. (The RF frequency times the circumference divided by c gives the number of buckets.)

FERMILAB'S ACCELERATOR CHAIN
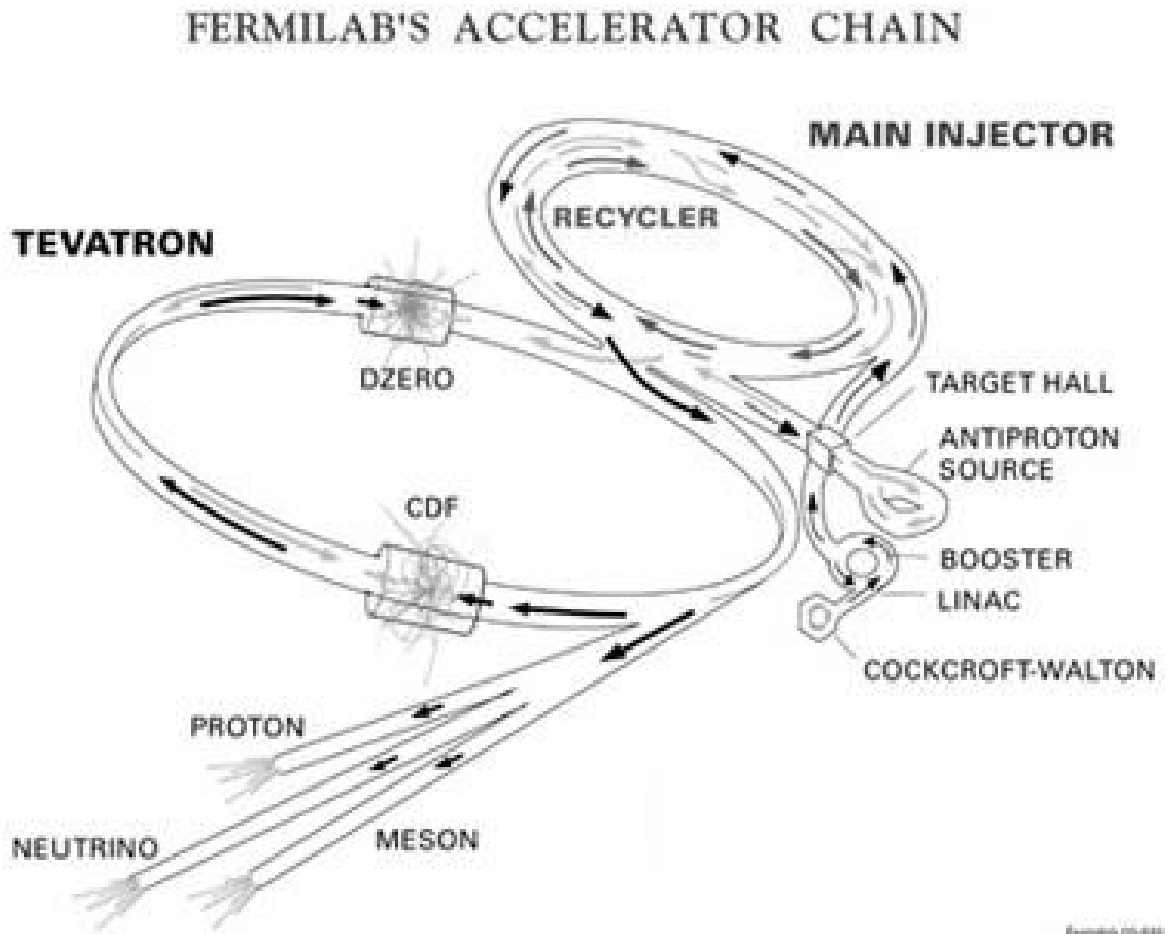
Figure 3.1: Illustration of Fermilab Accelerator Chain. The acceleration sequence begins in the Cockroft-Walton preaccelerator, goes through the Linac, then the Booster, into the Main Injector. From the Main Injector, particles can be accelerated and sent to the Tevatron or to the antiproton source target. CDF and DZero are the Tevatron's collision detector experiments, and the old Proton, Neutrino, and Meson fixed target experiment lines are also shown.

The Main Injector is typically filled with six separate 84-bunch batches from the Fermilab Booster accelerator. There are two empty buckets between each batch of 84, with a longer empty space after the final batch.

The amplitudes and decay characteristics of the wake magnetic fields used in the simulation were calculated by V. Kashikhin[6, 7] with OPERA-2D using the actual beam pipe and laminated iron core dipole magnet geometry. The field strength results from that modeling were then fit to a combination of two exponentials. For the horizontal dipole moment, (the direction which will kick the beam vertically), the fit of the Magnetic Wake Field after a dipole pulse of $1\mu s$ duration with each pole having $\pm 1Amp$ at $\pm 1mm$ offset from the center was found to be[3]:

$$B(t) = 1.612 \times 10^{-8} e^{(-t/49.2\mu s)} + 3.54 \times 10^{-9} e^{(-t/3.45\mu s)}$$

where B is given in Tesla.

The Main Injector dipole magnet beam pipe measures 6cm horizontally by 2.5cm vertically. This ellipticity means that the magnetic field induced by a vertical offset (the horizontal dipole field) will be greater than one caused the same offset in the horizontal plane, and an instability induced by a vertical beam offset will grow faster than a horizontal instability.

Unless noted otherwise, measurements and simulations in this thesis use the vertical axis displacements and the above horizontal dipole as their one dimension.

3.0.2 Main Injector Transverse Dampers

The Main Injector's transverse bunch position is detected with a stripline pickup. A hybrid transformer's difference output produces the position signal, which is a bipolar signal with amplitude proportional to the bunch position. It is digitized at 212 MHz, four times the bunch frequency, which allows the system to find the bunch phase and amplitude[4].
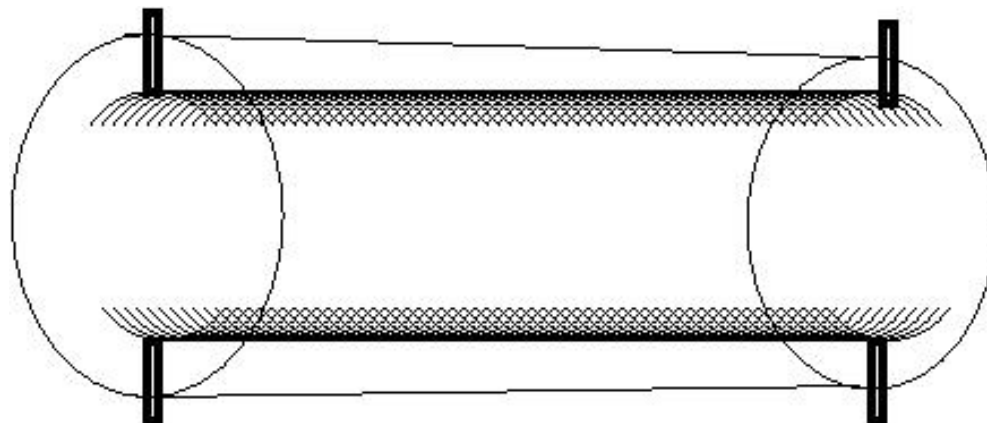
Figure 3.2: Illustration of the Damper system stripline detector or kicker.

The position detector and the damper kicker have similar stripline geometries as depicted in Figure 3.2. Both have parallel arched plates around an inner diameter of about 4 inches. For scale, the stripline cavity diameter is 6 inches. The kicker's plates are 40 inches long and each subtends 85 deg, while the pickup's plates are 12 inches long with arcs of 110 deg[2].

The transverse signals are one set of inputs to a single board digital damping system developed for the Fermilab Main Injector[4]. This damper board performs all the calculations for bunch-by-bunch transverse and longitudinal beam damping. At its heart is field-programmable gate array (FPGA) logic, outputting a digitally synthesized damping kick to power amplifiers. The term "bunch-by-bunch" means that the damping kick is calculated separately for each bunch. The damper card has analog inputs for the three dimensions of beam signals, A/D converters, the DAC output channels, and other digital inputs for beam clock and timing information.

The current transverse damper power amplifiers have enough power to induce a $0.1mm$ betatron oscillation in x for an 8.9 GeV/c beam. In the simulation, since the

kicker is idealized at the same position as the position readout, which has the same average beta value of roughly 26m for a typical tune around 24, this corresponds to a kick of on the order of $4.6\mu rad$. In the real damper system, since the kicker is at a position with a different beta, the actual amplitude in x' of the real kick is different. But the simulation kick has been calibrated to have the same effect as the damper kick.

3.1   Simulation Implementation

The simulation was implemented in Matlab, a mathematical programming language and environment. The simulation models one transverse dimension. Matlab vectors were constructed containing the charge, position (x), and position derivative with respect to longitudinal position $(x' = \frac{dx}{ds})$ for each of 588 bunches. As the simulation runs, x and x' propagate from each station to the next.

The accelerator circumference was similarly divided into 588 equidistant locations, or stations. The strength of the magnetic wakefield is tracked at each of those stations. The simulation runs by taking discrete time steps, the time it takes for each bunch to advance from one station to the next. This is simply the circumference divided by the number of stations (588) divided by βc, the speed of the beam, or approximately 18.8ns (which is, of course, the same as the bunch spacing).

In each time step, the simulation performs the following calculations:

1. The position of the bunch at the damper readout location is recorded.

2. The kick for the bunch at the damper kick location is calculated.

3. If damping is active, the bunch at the damper kick location receives the calculated kick in x'.

4. Each bunch gets kick in x' from its current station's magnetic wakefield

5. The magnetic field at each station decays

6. Each bunch deposits wake field at each station proportional to the bunch's charge and position

7. x and x' of each bunch propagate to the next station

8. The bunches (with their charge, x and x') advance in Z to the next stations

9. Time elapses

After each full turn (588 steps), the end-of-turn bunch positions are recorded in a vector for a time history of the beam evolution, and various maxima can be computed to show evolution of the beam as a whole.

3.2   Beam Pipe Diameter

The Main Injector beam pipe width only produces noticeable wakefield effects in the dipole magnets. In other parts of the circumference, the aperture is wide enough that any wakefield effects are negligible. Approximately 75% of the circumference has of the narrower diameter pipe. To simulate this, I use a "mask" vector with each element corresponding to one station, and for stations where that mask is 0, no wakefield deposition or kick occurs. 25% of the diameter of the Main Injector is thus masked off so that there are no wakefield effects.

The magnetic wake field is divided into two parts because the computed model indicates that the field is the sum of two separate exponential decays. Thus, the decays are computed separately, and the field which kicks the beam is the sum of the two parts.

Chapter 4

Simulation Results And Experimental Data

This chapter presents some of the results from the simulation.

4.1 Instability Growth

Figures 4.1 through 4.4 show the progression of the growth of a resistive wall instability using very simple input parameters for illustration purposes. Figure 4.1 shows the initial conditions. Six batches of 84 bunches each are set into the simulation. The first five batches all have ideal $x = 0$ positions. To simulate an injection error, the sixth batch has an x offset of 1mm. The bunch charge is identical for all bunches, corresponding to 5×10^{10} protons per bunch. After 100 turns, as shown in Figure 4.2, the effects of the injection error have begun to spread, and the betatron motion has begun to become apparent. The instability continues to grow, and as Figure 4.4 shows, it quickly blows up the whole beam.
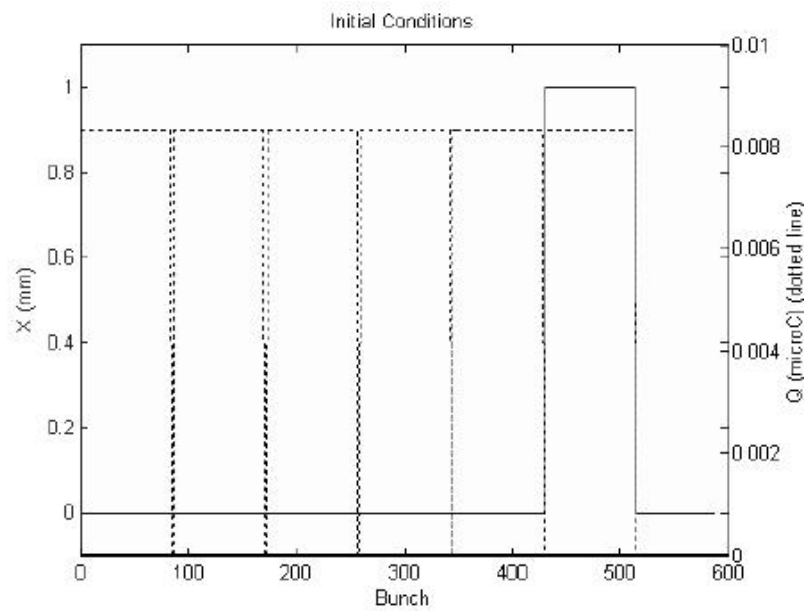
Figure 4.1: Initial Conditions for Instability Growth Demonstra-
tion. One batch has a 1mm position offset. All bunches
have equal charges.
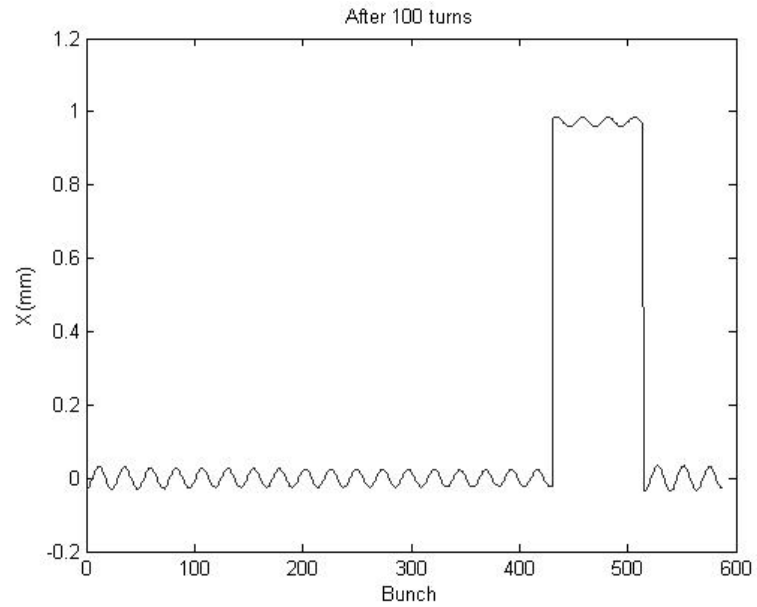
Figure 4.2: Bunch Positions after 100 Turn Simulation
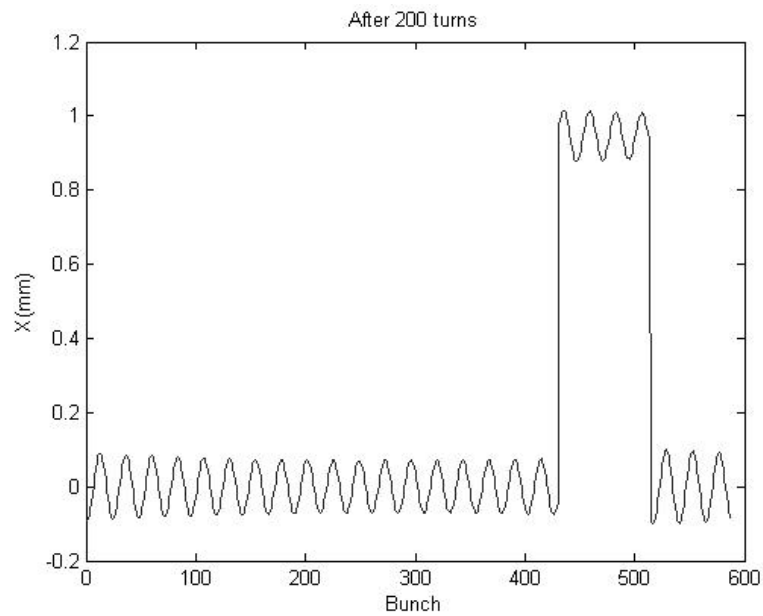
Figure 4.3: Bunch Positions after 200 Turn Simulation
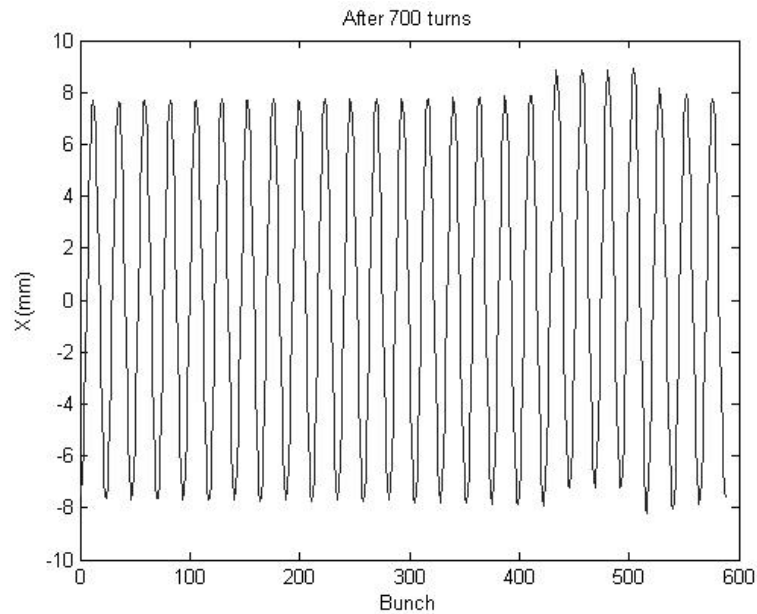
Figure 4.4: Bunch Positions after 700 Turn Simulation

4.2 Instability Growth Compared with Measurements

The simulation data was analyzed to measure the growth times of the instability. These measurements are compared with analysis of real Main Injector beam measurements which were also unstable.

4.3 Growth Measurements

Data to measure the instability growth time was acquired with the Main Injector digital damper system with the dampers off. All measurements are taken at a fixed, non-accelerating, beam energy. A sample of beam positions for some bunches in the same batch, is shown in Figure 4.5. In that figure, the position of each bunch is shown

as a separate trace. In Figure 4.6 the same data is shown with each trace plotted over the top of the others for 33 bunches. For analysis the maximum envelope across these 33 bunches is used as the indicator of the rise time of the instability. This maximum envelope is also shown in Figure 4.6. The maximum of the beam positions also plainly shows the point at which the beam starts scraping against the beam pipe, after about 900 turns.

The transverse dampers had been active during this experiment, and the dampers were turned off at turn number 50, relative to the start of this plot.

Figure 4.7 shows the initial conditions for the simulated beam. Five batches have no mean offset error, and the sixth batch of 84 bunches has a mean offset of 1mm. All the bunches have an initial random distribution of $\pm 0.5mm$ position. All the bunches an initial x' of zero and a charge of 5×10^{10} protons per bunch.

Figure 4.8 shows the end results of the simulation compared with the measured beam data. The Y axis shows logarithmic scaling here. The curve which is broader near Turn 0 is the simulated data. The "measurement" curve shows the maximum position envelope across the bunches in the same batch as described earlier. The "simulation" curve is created by taking the maximum position across all 84 bunches in batch 1. Both curves are then plotted as a function of turn number.

The two curves of Figure 4.8 are quite similar, neglecting the part of the measured curve after the beam starts physically scraping against its beam pipe around turn 900.

Each curve from Figure 4.8 was fit to an exponential function. Only the data between turns 300 and 800 was used, in order to avoid the beam scraping in the later turns and the earlier turns where the instability was still developing.

The results of the fit confirm the similarity in slope seen in Figure 4.8. The simulated data was proportional to $e^{0.0071t}$ and the measured data rose proportional to $e^{0.0073t}$.

For this experiment, a time bump was added to the beam trajectory near one of
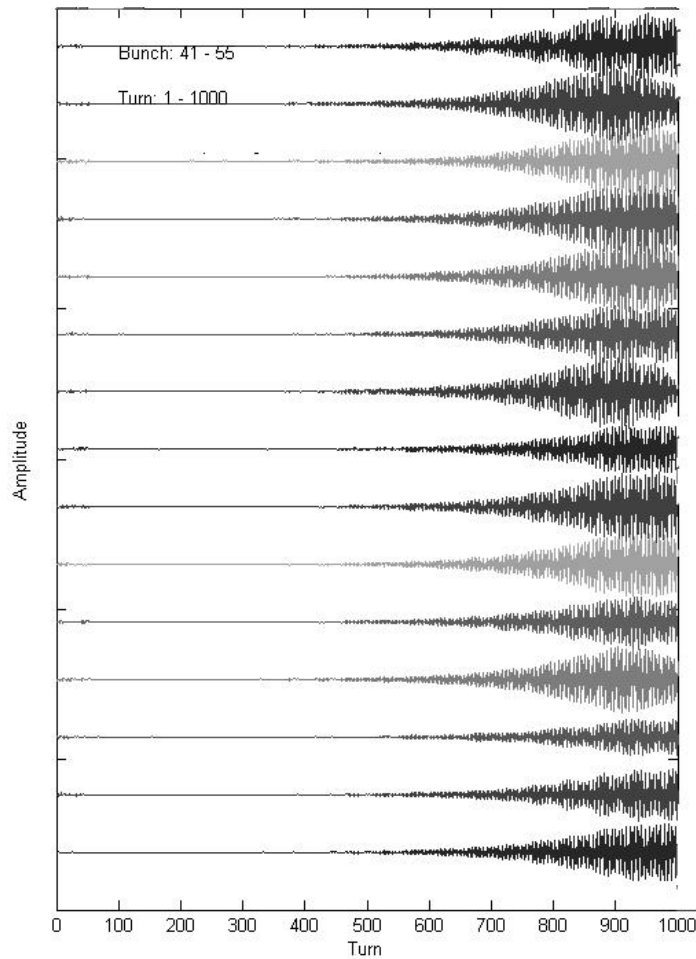
Figure 4.5: Position evolution over 1000 turns for 15 representative bunches. 8.9 GeV beam with damping initially on and damping turned off after turn 50. The maximum amplitude of each bunch's curve is the beam pipe radius, $\pm 2.5 cm$.
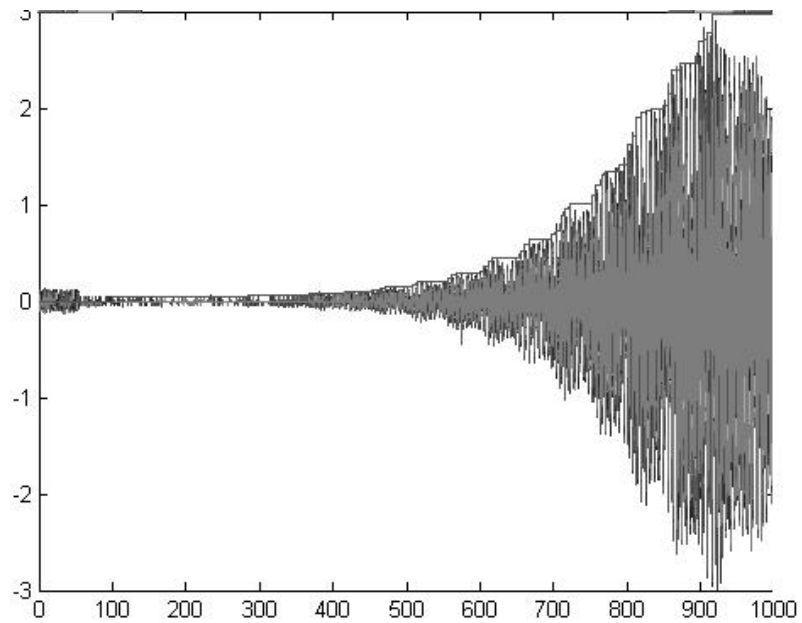
Figure 4.6: Bunch Position Evolution over 1000 turns. Same data as the previous figure, but with curves for all bunches drawn on top of one another and an additional curve indicating maximum envelope across bunches. Again the maximum scale is $\pm 2.5 cm$ since the bunches scrape against the beam pipe at about turn 900.
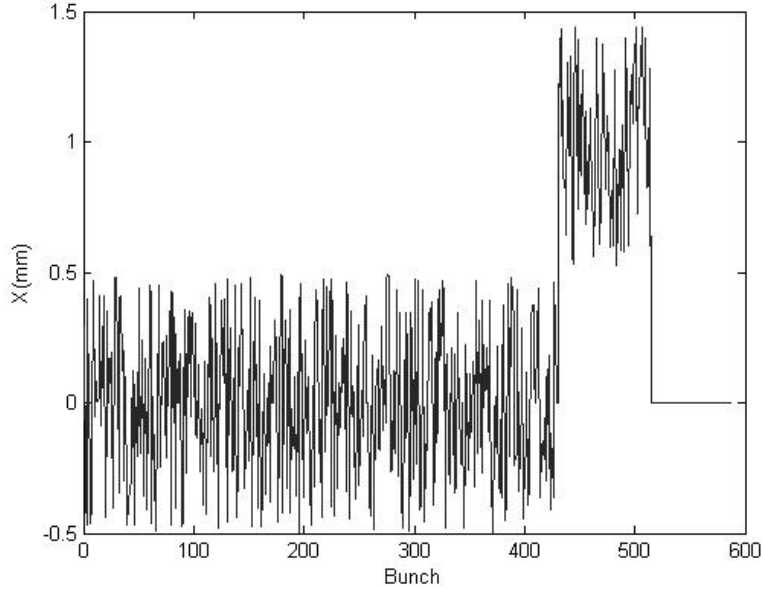
Figure 4.7: Initial Bunch Positions For Simulation

the Main Injector Lambertson magnets to test any effect of moving the beam near the septum. Bumps were tried of amplitude $-.3, -0, 4, -0.45$, and $+.5$ Amps of current to the corrector magnets, corresponding to motions of roughly 3, 4, and 5 mm toward the septum and 5mm away from the septum relative to the nominal beam position. These changes did not appear to make any significant difference in the instability growth. These amplitudes were enough to move the beam significantly but retained a safety margin so as to not scrape the beam into the magnet septum. The variations in these bumps and the corresponding proximity to the septum did not have any appreciable effect on the growth time of the instability. This is shown in the log plots of Figure 4.9. Fitting the rise times to an exponential showed that all four curves rose proportional to between $e^{0.0071t}$ and $e^{0.0073t}$. This means the amplitude of the instability doubles about every 97 turns, by solving $\frac{x_2}{x_1} = 2 = \frac{e^{0.0071t_2}}{e^{0.0071t_1}}$ for $t_2 - t_1$.
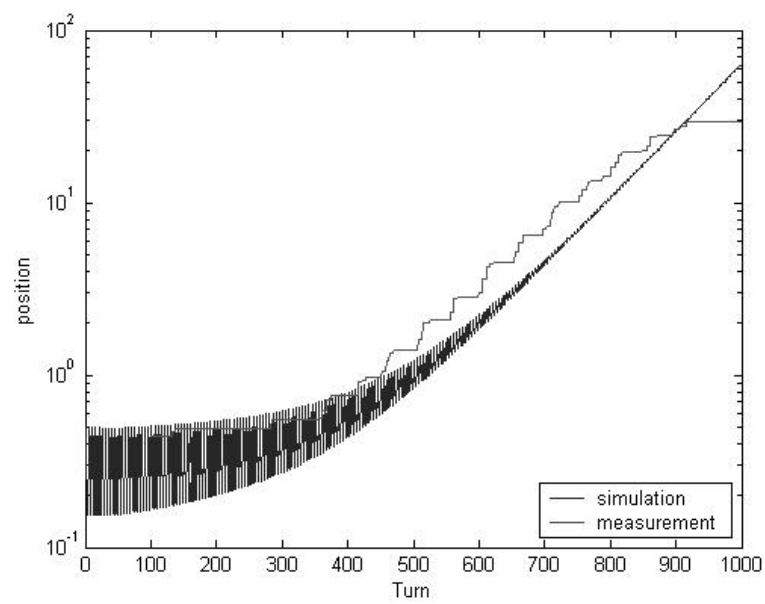
Figure 4.8: Transverse Displacement Maximum Across Bunches Evolving Through Time (Turns) — Simulated and Measured. The Y axis is in millimeters, but arbitary data acquisition units from the beam data were scaled to match the other curve.
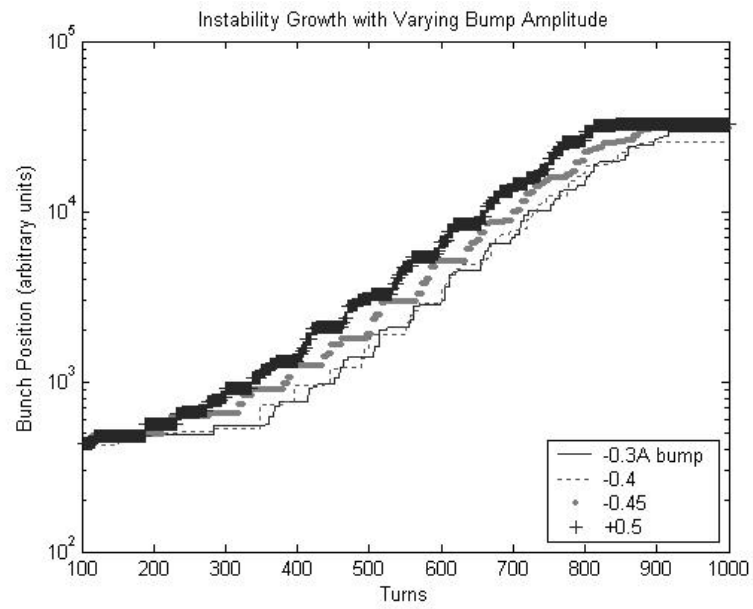
Figure 4.9: Instability growth for varying orbit bumps which moved the beam roughly $\pm 5mm$

Chapter 5

Damping

As indicated previously, the simulation includes simulation of a damping kick which can produce a 0.1mm transverse displacement after a quarter of a betatron oscillation. The position for the kick is sensed at one position and the kick is applied at one position. For the purposes of these simulations, the readout and kick position are the same, although in practice, they are not at the exact same location. The same algorithm that is used in the FPGA for calculating the damping kick is used in the simulation. This includes a calculation of the bunch motion phase.

Consider the analogy of a person on a swing. If you push them forward while they are still in the backwards motion part of the swing, that will lessen the height of their swing. Conversely, if you push them forwards while they are moving forwards, an in-phase push, then you will increase the height of their swing.

The same principles apply with beam damping. Applying a kick out-of-phase with the particle oscillations will diminish the amplitude of the oscillation. This is the damping process. Applying a kick in-phase with the particle motion will increase the oscillation amplitude of the particle, and this is anti-damping, or pinging, the beam.
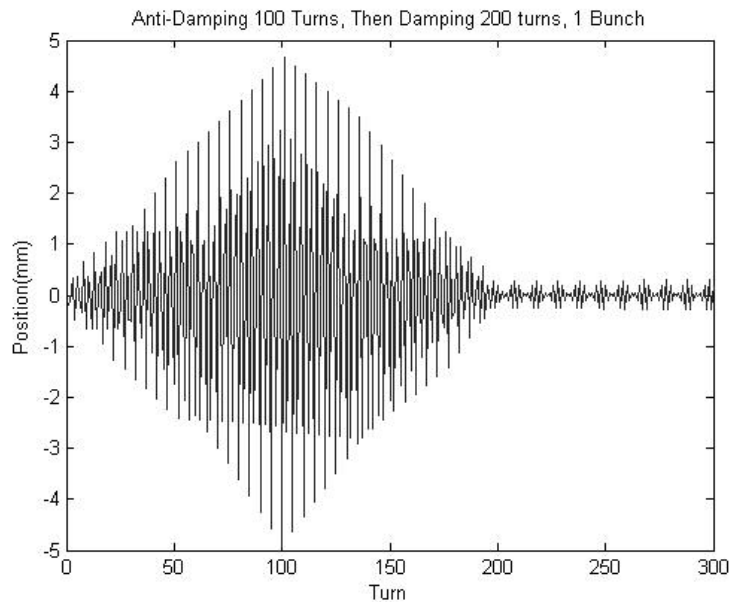
Figure 5.1: Maximum Bunch Position, Anti-Damping for 100
turns, then Damping

5.1 Anti-Damping and Damping

For this simulation, starting conditions were: 5×10^{10} protons per bunch, $\nu = 24.4$,
five batches of 84 bunches with no initial position offset, and the sixth batch of 84
with an initial position offset error of 1mm.

Figure 5.1 shows the maximum bunch position across the 84 bunches of batch #1
measured for 200 turns. The damping kick was turned on for the entire simulation,
but for the first 100 turns, the phase of the dampers was adjusted to provide anti-
damping — encouraging the beam position oscillations to grow faster than normal.
For the second 100 turns, the phase was changed to the optimal phase to provide
damping. Figure 5.1 clearly shows the beneficial effects of damping to control the
beam oscillations.

5.2 Bunch-by-Bunch Coefficients

Both the simulation and the Main Injector digital damper card provide the ability to provide a different kick to each bunch of the beam. For ordinary damping, this allows each bunch to be damped according to its individual betatron amplitude and phase. However, this also allows us to select certain bunches for anti-damping by changing the phase of the damper kick for those bunches. This allows a more exotic bunch structure to be created. Figures 5.2 and 5.3 illustrate the results of one simulation run with selective anti-damping. Figure 5.3 shows the evolution of bunch positions over 200 turns for the anti-damped bunch and two bunches on either side of it. Figure 5.3 shows the ending bunch positions after 200 turns through the Main Injector. The kick phase for bunch 5 was 180 deg out of phase with the other bunches with the effect that bunch 5 is ejected from the beam. These simulation results are very similar to the results shown for selective anti-damping demonstrated by the digital damper card in 2003[4].

5.3 Varying Beam Charge

One of the key advantages of the Main Injector digital damper system is that the damping enables the Main Injector to use a more intense beam, which provides more luminosity to the Fermilab experiments. Without transverse dampers, the more intense beams become unstable too quickly.

With only 5×10^9 protons per bunch the simulation shows no noticeable instability growth after 1000 turns starting with a beam that had a random bunch x offset of $\pm 0.25mm$. There is not enough charge per bunch to accumulate a significant magnetic wake field. Figure 5.4 compares the instability growth times for beams with 5×10^{10}, 5×10^{11}, and 1×10^{12} protons per bunch. Starting position offsets were randomly
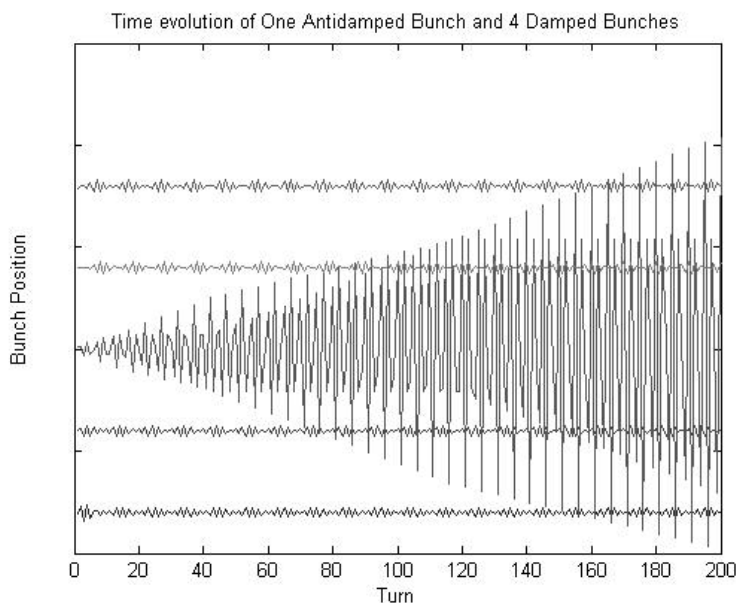
Figure 5.2: Selective Anti-Damping Time Evolution, 5 Bunches

distributed over $\pm 0.25mm$. Again in this figure, each point plotted was taken from the maximum position across the first 84 bunches after each turn. For these cases, the tune was 24.2313, and the initial x offset was $\pm 0.25mm$ per bunch.

All the curves in Figure 5.4 are with damping turned off. With damping on the damper system is able to squelch the wakefield instability at both the 5×10^{10} and 5×10^{11} intensity. Figure 5.5 is the simulation results that show the dampers control the growth of the instability at 5×10^{11} protons/bunch. As in the other figures, Figure 5.5 plots the maximum transverse position across the first 84 bunches after each turn.

However, at 10^{12} protons per bunch, the beam always blows up after just a few turns in the simulation. This implies that the $0.1mm$ kick of the currently modeled and deployed amplifiers would not have enough power to control that beam.

Fermilab's Run II design goal is to use 5×10^{12} protons per *batch* of 84 bunches,
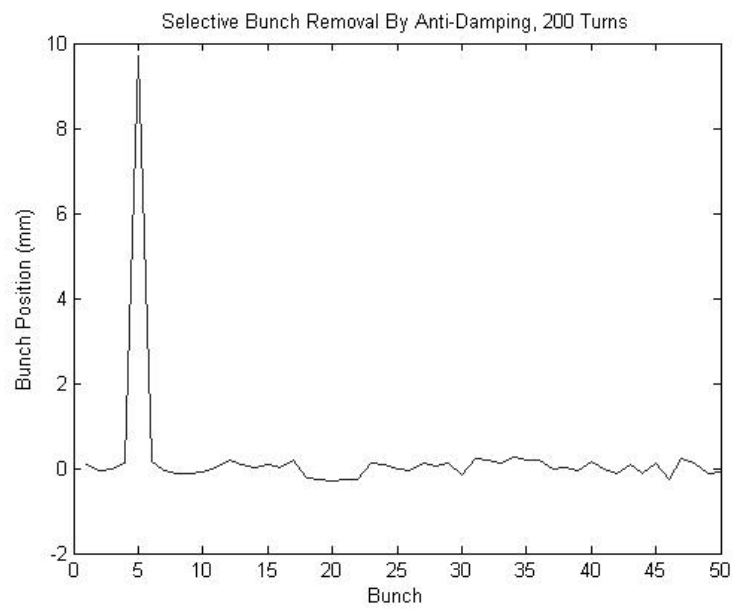
Figure 5.3: Selective Anti-Damping, Bunch Positions after 200 turns, same data as the previous figure
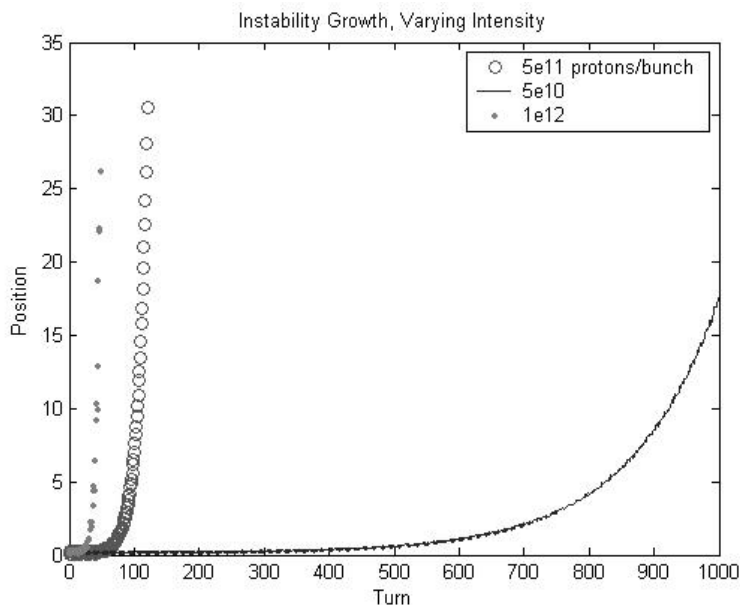
Figure 5.4: Instability Growth with Varying Bunch Intensities

or about 6×10^{10} protons per bunch. So this simulation shows the current dampers will be more than adequate for those intensities.

5.4 Horizontal vs. Vertical Instability Growth

As noted previously, the Main Injector beampipe is wider than it is high, implying that a vertical instability should grow faster than a horizontal one. This is demonstrated by beam measurements taken and shown in Figures 5.6 and Figures 5.7. For these figures, the beam position was measured both horizontally and vertically, and the maximum position envelope across bunches was taken as in Section 4.3.

In Figure 5.6, the horizontal dampers were turned off and the vertical dampers were left on and the horizontal instability grows at a rate proportional to $e^{0.004821t}$ (doubling in amplitude ever 144 turns). In Figure 5.7, when the vertical dampers
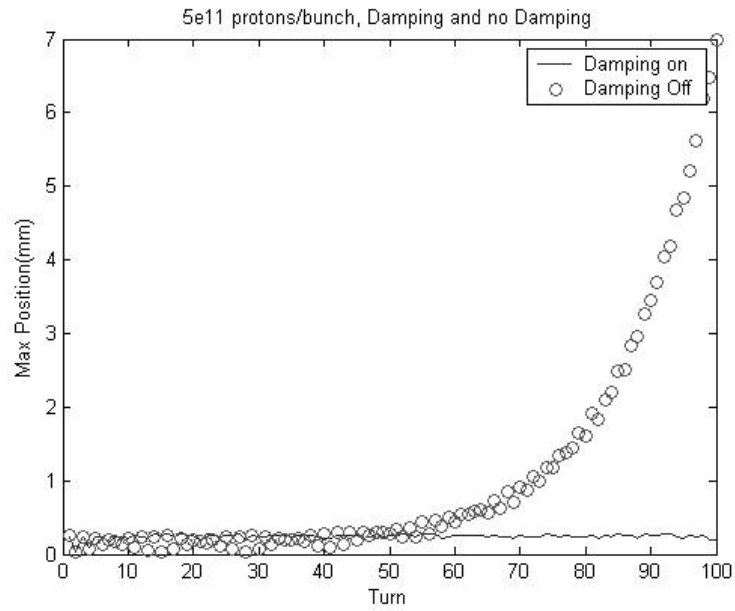
Figure 5.5: 5×10^{11} Protons per Bunch with Damping On and Off
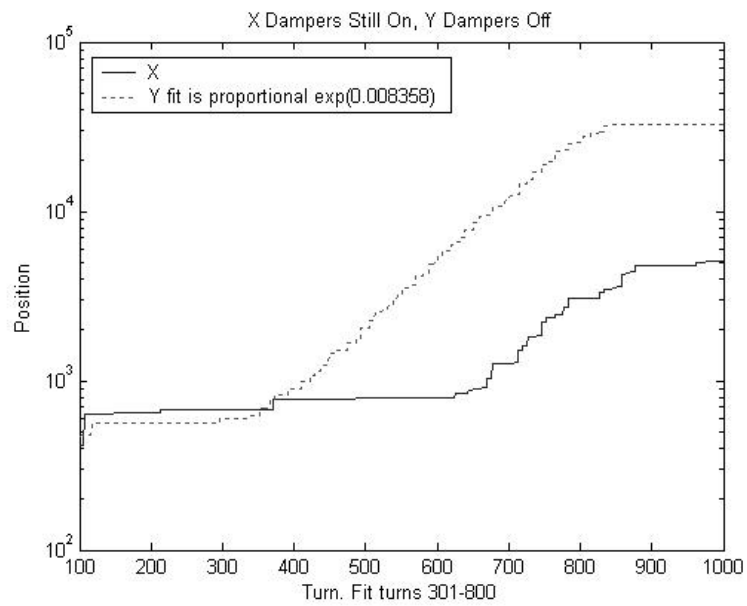
were turned off and the horizontal dampers were left on, the vertical instability grows at a rate proportional to $e^{0.008358t}$ (doubling every 83 turns).
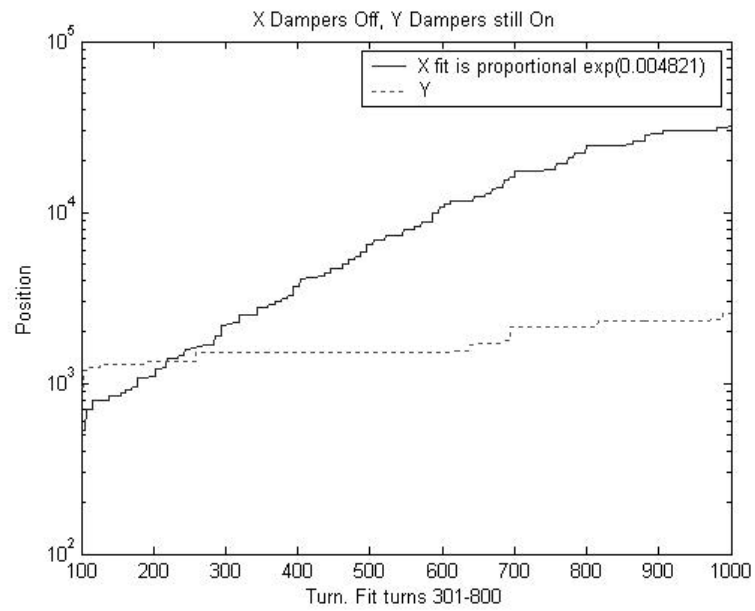
Figure 5.6: X Dampers Off, X Instability Amplitude doubles in 144 Turns

Figure 5.7: Y Dampers Off, Y Instability Amplitude doubles in 83

Turns

Chapter 6

Conclusions

This rigid bunch simulation has proven to be a useful tool for understanding the behavior of the beam in the Fermilab Main Injector. The simulation also is a useful aid to understanding the Main Injector digital bunch-by-bunch damper card, the need for such damping, its performance, and its capabilities.

Use of a rigid bunch approximation is one limitation to this simulation. Use of rigid bunches does not allow it to account for finite chromaticity which spreads the frequencies of the orbiting particles and can wash out the growth of wakefield instabilities. This property is used to allow the Main Injector to function at relatively high intensities without any damping. However, to go to desired higher intensities, damping is needed. Another limitation is that the beam positions are allowed to go to infinity rather than being clipped at the diameter of the beam pipe where the particles would be scraped away. This last limitation would be a straightforward change to the simulation code.

Appendix A

Simulation Calibration Procedures

To demonstrate that the basics of the calibration were correct, some simple operations were performed which could be compared with easily computed expected values. This appendix contains a list of those checks.

1. The transfer matrix which advances x and x' from one station to the next was checked. For this check, x and x' are set to a set of simple patterns, for instance $x = 0, x' = 1$, and the system is advanced to the next station. We were able to easily check that the values at the next station were correct.

2. After integral number of tunes, the beam x and x' are back where they started. To show this, an initial pattern was set for the bunches in x and x', the wakefield deposition, decay, and kick were turned off, and the beam was put through a number of turns N so that $N\nu$ is an integer. For instance, with the beam tune $\nu = 24.4$, the bunches are advanced through 5 turns, and the resulting x and x' was observed to be the same as the initial conditions.

3. The value of the magnetic wakefield was compared with its expected value. This was done by setting the number of particles in a bunch to 1.2×10^{13} to

get $2\mu C$ per bunch, then observing that the induced magneting field matched the amplitude predicted by the input model. The magnetic field made to decay for lengths of time and the amplitude in the simulation matched the predicted values.

4. With a starting condition of one bunch stepped around the ring, the simulation produced the expected betatron oscillation pattern.

5. The Fermilab Main Injector transverse damper power amplifiers have enough power to induce a $0.1mm$ kick to the beam. To verify the simulation had the correct damper kick strength, all the charge deposition, decay, and resistive-wall kick features were turned off, and one bunch was kicked by the damper one time. After one-quarter period of betatron oscillation, the bunch is observed to have the expected 0.1mm betatron oscillation amplitude.

Bibliography

[1] D. A. Edwards and M. J. Syphers, *An Introduction to the Physiscs of High Energy Accelerators* John Wiley & Sons, New York, 1993.

[2] Fermilab Technical Drawing Numbers 0430.030-MD-260677 and 0430.030-MD-260687 for Kicker and Detector Striplines.

[3] G. William Foster, *Wake Field Excel Spreadsheet* Unpublished excel file, 2003.

[4] G. William Foster, Sten Hansen, Dennis Nicklaus, Warren Schappert, Alexei Seminov, Dave Wildman, and W. Ashmanskas, *Bunch-By-Bunch Digital Dampers for the Fermilab Main Injector and Recycler* Particle Accelerator Conference, 2003

[5] Gerald P. Jackson, *The Effect of Chromatic Decoherence on Transverse Injection Oscillation Damping* Published Proceedings of Technical Workshop on *Feedback Control of Multi-Bunch Instabilities in Proton Colliders at the Highest Energies and Luminosities*, Erice, Sicily, 1992. Fermilab Document Fermilab-Conf-93/010.

[6] V. S. Kashikhin, *Wake Magnetic Field Analysis.* Unpublished memo, May 30, 2003.

[7] V. S. Kashikhin, *Wake Magnetic Field Analysis.* Unpublished memo including Vertical Dipole Field and Horizontal Dipole Field, Feb. 27, 2004.

[8] S. Koscielniak and H. J. Tran, *Properties of a Transverse Damping System, Calculated by a Simple Matrix Formalism.* Proceedings of the 1995 IEEE Particle Accelerator Conference, Dallas Texas, May 1-5 1995.

[9] S. Y. Lee, *Accelerator Physics.* World Scientific Publishing Co., Singapore, 1999.

[10] C. Y. Tan and J. Steimel, *The Tevatron Transverse Dampers.* In *Proceedings of the 2003 Particle Acclerator Conference,* Portland, OR, 2003.

[11] C. S. Taylor *Microwave Kickers and Pickups* in *Oxford 1991, Proceedings, RF engineering for particle accelerators, vol. 2*, 458-473. CERN Geneva - CERN-92-03.x

[12] Bruno W. Zotter and Semyon A. Kheifets, *Impedances and Wakes in High-Energy Particle Accelerators.* World Scientific Publishing Co., Singapore, 1998.

[13] V.M. Zhabitsky, *Transverse Feedback System with a Digital Filter and Additional Delay,* Proceedings of the 1986 European Particle Accelerator Conference, p. 1833, 1986.